



# Inflammation and the Nervous System: The Connection in the Cornea in Patients with Infectious Keratitis

## Citation

Cruzat, Andrea, Deborah Witkin, Neda Baniyasadi, Lixin Zheng, Joseph B. Ciolino, Ula V. Jurkunas, James Chodosh, Deborah Pavan-Langston, Reza Dana, and Pedram Hamrah. 2011. "Inflammation and the Nervous System: The Connection in the Cornea in Patients with Infectious Keratitis." *Investigative Ophthalmology & Visual Science* 52 (8) (July 11): 5136. doi:10.1167/iovs.10-7048.

## Published Version

10.1167/iovs.10-7048

## Permanent link

<http://nrs.harvard.edu/urn-3:HUL.InstRepos:34387112>

## Terms of Use

This article was downloaded from Harvard University's DASH repository, and is made available under the terms and conditions applicable to Other Posted Material, as set forth at <http://nrs.harvard.edu/urn-3:HUL.InstRepos:dash.current.terms-of-use#LAA>

## Share Your Story

The Harvard community has made this article openly available.  
Please share how this access benefits you. [Submit a story](#).

[Accessibility](#)

# Inflammation and the Nervous System: The Connection in the Cornea in Patients with Infectious Keratitis

Andrea Cruzat,<sup>1,2</sup> Deborah Witkin,<sup>1</sup> Neda Baniasadi,<sup>1,2</sup> Lixin Zheng,<sup>1</sup> Joseph B. Ciolino,<sup>2</sup> Ula V. Jurkunas,<sup>2</sup> James Chodosh,<sup>2</sup> Deborah Pavan-Langston,<sup>2</sup> Reza Dana,<sup>2</sup> and Pedram Hamrah<sup>1,2</sup>

**PURPOSE.** To study the density and morphologic characteristics of epithelial dendritic cells, as correlated to subbasal corneal nerve alterations in acute infectious keratitis (IK) by in vivo confocal microscopy (IVCM).

**METHODS.** IVCM of the central cornea was performed prospectively in 53 eyes with acute bacterial ( $n = 23$ ), fungal ( $n = 13$ ), and *Acanthamoeba* ( $n = 17$ ) keratitis, and in 20 normal eyes, by using laser in vivo confocal microscopy. Density and morphology of dendritic-shaped cells (DCs) of the central cornea, corneal nerve density, nerve numbers, branching, and tortuosity were assessed and correlated. It should be noted that due to the "in vivo" nature of the study, the exact identity of these DCs cannot be specified, as they could be monocytes or tissue macrophages, but most likely dendritic cells.

**RESULTS.** IVCM revealed the presence of central corneal DCs in all patients and controls. The mean DC density was significantly higher in patients with bacterial ( $441.1 \pm 320.5$  cells/mm<sup>2</sup>;  $P < 0.0001$ ), fungal ( $608.9 \pm 812.5$  cells/mm<sup>2</sup>;  $P < 0.0001$ ), and *Acanthamoeba* keratitis ( $1000.2 \pm 1090.3$  cells/mm<sup>2</sup>;  $P < 0.0001$ ) compared with controls ( $49.3 \pm 39.6$  cells/mm<sup>2</sup>). DCs had an increased size and dendrites in patients with IK. Corneal nerves were significantly reduced in eyes with IK compared with controls across all subgroups, including nerve density ( $674.2 \pm 976.1$  vs.  $3913.9 \pm 507.4$   $\mu\text{m}/\text{frame}$ ), total nerve numbers ( $2.7 \pm 3.9$  vs.  $20.2 \pm 3.3$ ), main trunks ( $1.5 \pm 2.2$  vs.  $6.9 \pm 1.1$ ), and branching ( $1.2 \pm 2.0$  vs.  $13.5 \pm 3.1$ ;  $P < 0.0001$ ). A strong association between the

diminishment of corneal nerves and the increase of DC density was observed ( $r = -0.44$ ;  $P < 0.0005$ ).

**CONCLUSIONS.** IVCM reveals an increased density and morphologic changes of central epithelial DCs in infectious keratitis. There is a strong and significant correlation between the increase in DC numbers and the decreased subbasal corneal nerves, suggesting a potential interaction between the immune and nervous system in the cornea. (*Invest Ophthalmol Vis Sci.* 2011;52:5136–5143) DOI:10.1167/iovs.10-7048

Corneal nerves are of great interest to clinicians and scientists, because of their important roles in regulating corneal sensation, epithelial integrity, proliferation, wound healing, and for their protective functions.<sup>1,2</sup> The cornea is a densely innervated tissue supplied by the terminal branches of the ophthalmic division of the trigeminal nerve as ciliary nerves.<sup>3</sup> Corneal nerves penetrate the corneal periphery in a radial distribution, parallel to the superficial corneal surface, between the Bowman's layer and the basal epithelium, configuring the subbasal nerve plexus that supplies the overlying corneal epithelium.<sup>3</sup>

In vivo confocal microscopy (IVCM) is a noninvasive procedure that allows imaging the living cornea at the cellular level, providing images comparable with histochemical methods. IVCM enables the study of corneal cells, nerves, and the immune cells in different ocular and systemic diseases, and after corneal surgery.<sup>4,5</sup> The complex stromal and epithelial branching of corneal nerves is not visible by conventional slit-lamp biomicroscopy, but can be visualized by IVCM.

Our group has recently demonstrated the loss of corneal sensation in patients with herpes simplex keratitis (HSK), which is strongly correlated with the profound diminishment of the subbasal nerve plexus in these patients by IVCM with a slit scanning confocal microscope (Confoscan 4; Nidek Inc., Gamagori, Japan).<sup>6</sup> Furthermore, IVCM revealed that the loss of the subbasal nerve plexus started within days of acute HSK onset. More recently, we also observed a profound diminishment of the subbasal corneal nerve plexus in a pilot study of patients with fungal and *Acanthamoeba* keratitis by laser IVCM, where we observed the close proximity and apposition of subbasal nerves with epithelial dendritic cells in the cornea (Kurbanyan K, et al. *IOVS* 2009;50:ARVO E-Abstract 2402).

Dendritic cells, the most potent antigen-presenting cells (APCs) of the body, are strategically positioned as immune sentinels ready to respond to invading pathogens in peripheral tissues.<sup>7</sup> Dendritic cells have been shown to be critical for the initiation of adaptive immune responses and for maintenance of peripheral tolerance. Dendritic cells also represent the principal immune sentinels to the foreign world in the cornea and ocular surface (reviewed in Refs. 8 and 9). While central corneal dendritic cells were initially described in mice,<sup>10–12</sup> their presence has now been confirmed in humans, both by ex vivo

From the <sup>1</sup>Ocular Surface Imaging Center and <sup>2</sup>Cornea and Refractive Surgery Service, Massachusetts Eye & Ear Infirmary, Department of Ophthalmology, Harvard Medical School, Boston, Massachusetts.

Presented in part at the Biennial Cornea Research Conference, Boston, Massachusetts, October 2009, and at the annual meeting of the Association of Research in Vision and Ophthalmology, Fort Lauderdale, Florida, May 2010.

Supported by NIH K12-EY016335 (PH), NIH K08-EY020575 (PH), NIH K24-EY19098 (RD), New England Corneal Transplant Research Fund (PH), Falk Medical Research Foundation (PH), and an unrestricted grant to the Department of Ophthalmology, Harvard Medical School, from Research to Prevent Blindness, New York, New York. The funding organizations had no role in the design or conduct of this research.

Submitted for publication December 13, 2010; revised February 8, and March 19, 2011; accepted March 26, 2011.

Disclosure: A. Cruzat, None; D. Witkin, None; N. Baniasadi, None; L. Zheng, None; J.B. Ciolino, None; U.V. Jurkunas, None; J. Chodosh, None; D. Pavan-Langston, None; R. Dana, None; P. Hamrah, None

Corresponding author: Pedram Hamrah, Ocular Surface Imaging Center, Cornea and Refractive Surgery Service, Massachusetts Eye & Ear Infirmary, Harvard Medical School, 243 Charles Street, Boston, MA 02114; pedram\_hamrah@meci.harvard.edu.

studies<sup>13–15</sup> and more recently by IVCN at the level of the basal epithelium and Bowman's layer in the central cornea.<sup>16–18</sup>

Previous studies in the skin and gut literature have demonstrated the bidirectional interplay of the immune and nervous system.<sup>19–21</sup> Further, experimental studies have shown the immunomodulatory function of nerves via neuropeptides in mice.<sup>20–22</sup> In the present study, our aim was to evaluate the density and morphologic characteristics of epithelial dendritic-shaped cells (DCs) and to correlate them to the subbasal corneal nerve alterations by laser IVCN in a prospective fashion in patients with infectious keratitis (IK). Although tissue macrophages or monocytes can have this morphology, we attributed the dendritic-shaped cells to dendritic cells. Our data demonstrates that diminishment of the subbasal nerve plexus in IK significantly correlates with the increase of epithelial DC density in these patients.

## PATIENTS AND METHODS

We conducted a prospective, cross-sectional study, in a controlled, single-blinded fashion. Fifty-three eyes of 53 patients with diagnosis of acute infectious bacterial, fungal, and *Acanthamoeba* keratitis were included in the study. Twenty eyes of 20 normal volunteers constituted the control group. All subjects were recruited from the Cornea Service of the Massachusetts Eye & Ear Infirmary, Boston, Massachusetts, between 2009 and 2010. This study was Health Insurance Portability and Accountability Act (HIPAA)-compliant, adhered to the tenets of the Declaration of Helsinki, and was approved by the Institutional Review Board (IRB)/Ethics Committee of our institution. Written informed consent was obtained from all subjects after a detailed explanation of the nature of the study. All patients and normal subjects underwent slit-lamp biomicroscopy. Patients were diagnosed with acute infectious keratitis according to the clinical history and clinical examination. Only patients with positive corneal cultures or positive confocal findings for fungal or *Acanthamoeba* keratitis were included. Duration of disease was included from the time patients presented with clinical evidence of infectious keratitis. The study excluded subjects with a history of any prior episode of infectious keratitis, ocular inflammatory disease, ocular trauma, previous eye surgery within 3 months, or diabetes. Patients receiving local or systemic corticosteroid therapy at the time of the examination were not included.

Laser scanning in vivo confocal microscopy (Heidelberg Retina Tomograph 3 with the Rostock Cornea Module, Heidelberg Engineering GmbH, Dossenheim, Germany) of the central cornea was performed in all subjects. This microscope uses a 670-nm red wavelength diode laser source and it is equipped with a 63 $\times$  objective immersion lens with a numerical aperture of 0.9 (Olympus, Tokyo, Japan). The laser confocal microscope provides images that represent a coronal

section of the cornea of 400  $\times$  400  $\mu\text{m}$ , which is 160,000  $\mu\text{m}^2$ , at a selectable corneal depth and is separated from adjacent images by approximately 1 to 4  $\mu\text{m}$ , with a lateral resolution of 1  $\mu\text{m}$ /pixel. Digital images were stored on a computer workstation at 30 frames per second. A disposable sterile polymethylmethacrylate cap (Tomo-Cap; Heidelberg Engineering GmbH, Dossenheim, Germany), filled with a layer of hydroxypropyl methylcellulose 2.5% (GenTeal gel; Novartis Ophthalmics, East Hanover, NJ) in the bottom, was mounted in front of the cornea module optics for each examination. One drop of topical anesthesia 0.5% proparacaine hydrochloride (Alcaine; Alcon, Fort Worth, TX) was instilled in both eyes, followed by a drop of hydroxypropyl methylcellulose 2.5% (GenTeal gel, Novartis Ophthalmics) in both eyes. One drop of hydroxypropyl methylcellulose 2.5% was also placed on the outside tip of the cap to improve optical coupling, and manually advanced until the gel contacted the central surface of the cornea.

A total of six to eight volume and sequence scans were obtained from the center of each cornea, at least three of which were sequence scans with particular focus on the subepithelial area, the subbasal nerve plexus, and epithelial dendritic cells, typically at a depth of 50 to 80  $\mu\text{m}$  (Fig. 1). When a corneal ulcer was present with an epithelial defect, both the ulcer and the surrounding area were scanned and analyzed. A minimum of three representative images of the subbasal nerve plexus and epithelial dendritic cells were selected for analysis for each eye. The images were selected from the layer immediately at or posterior to the basal epithelial layer and anterior to the Bowman's layer. The criteria to select the images were the best focused and complete images, with the whole image in the same layer, without motion, without folds, and good contrast.

Three masked observers evaluated the confocal images for central corneal DC density, DC size, number of dendrites per cell, corneal nerve morphology, and analyzed the subbasal nerve plexus as previously described.<sup>6,22</sup> IVCN images at a depth of 50 to 70  $\mu\text{m}$  at the level of basal epithelial layers, basal lamina, or subbasal nerve plexus were chosen for analysis of DCs. It should be noted that due to the "in vivo" nature of the study, the exact identity of these DC cannot specified, as they could be monocytes or tissue macrophages, but most likely dendritic cells. DCs were morphologically identified as bright individual dendritiform structures with cell bodies that allowed us to differentiate these structures from the corneal nerves. Briefly, DCs were counted using software (Cell Count, Heidelberg Engineering GmbH) in the manual mode. The data were expressed as density (cells/ $\text{mm}^2$ )  $\pm$  SD. DC size and number of dendrites per DC were analyzed using ImageJ software (developed by Wayne Rasband, National Institutes of Health, Bethesda, MD; available at <http://rsb.info.nih.gov/ij/>). DC size was measured as the area covered by a single cell. The data were expressed as size ( $\mu\text{m}^2$ )  $\pm$  SD and dendrites per cell  $\pm$  SD. The nerve analysis was done using the semi-

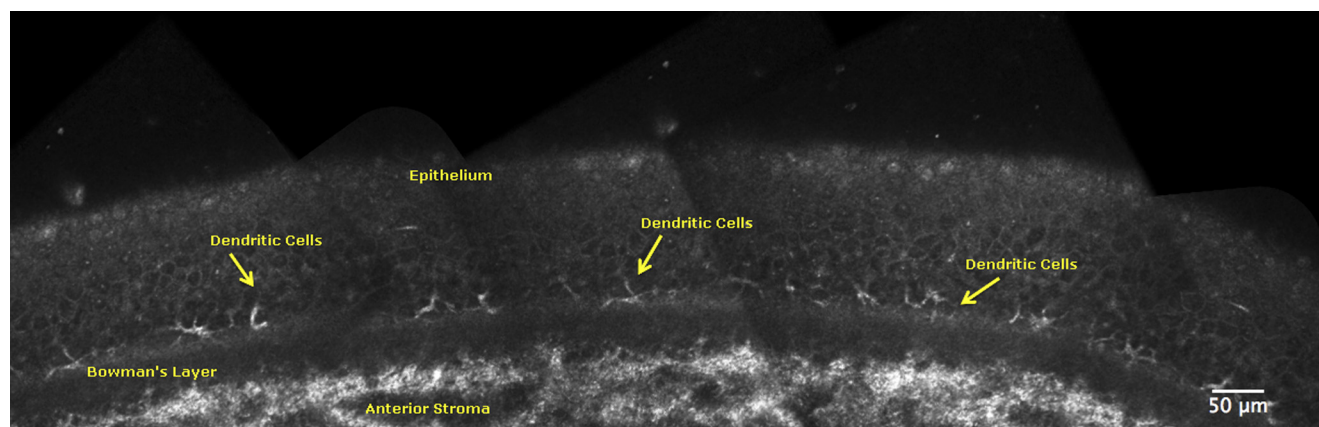


**FIGURE 1.** Oblique section through corneal epithelium, basal membrane, and anterior stroma in bacterial keratitis. Epithelial dendritic cells (yellow arrows) were visualized in the basal epithelial layer and subbasal nerve plexus.

TABLE 1. Demographic Data of Normal Controls and Patients with Infectious Keratitis

	Controls	Bacterial Keratitis	Fungal Keratitis	Acanthamoeba Keratitis
Patients, <i>n</i>	20	23	13	17
Age, y	33.1 ± 7.6	36.3 ± 13.2	48.8 ± 18.4	36.5 ± 14.1
Sex, male/female	10/10	12/11	9/4	9/8
Days of infection	—	8.9 ± 6.9	16.1 ± 18.3	15.5 ± 12.4
Contact lens use, %	0	78.3	30.8	68.7

Values are mean ± SD except where otherwise noted. Days of infection is time elapsed since diagnosis of the infection until the in vivo confocal microscopy was performed.

automated tracing program NeuronJ,<sup>23</sup> a plug-in for ImageJ (<http://www.imagescience.org/meijering/software/neuronj/>; see Fig. 3O). Nerve density was assessed by measuring the total length of the nerve fibers in micrometers per frame (160,000  $\mu\text{m}^2$ ). Main nerve trunks were defined as the total number of main nerve trunks in one image after analyzing the images anterior and posterior to the analyzed image to confirm that these did not branch from other nerves. Nerve branching was defined as the total number of nerve branches in one image. The number of total nerves measured was defined as the number of all nerves, including main nerve trunks and branches in one image. The grade of nerve tortuosity was classified in four grades according to a tortuosity grading scale reported by Oliveira-Soto and Efron.<sup>24</sup> Statistical analysis was performed by Student's *t*-test and ANOVA to compare the different groups. The Pearson correlation coefficient was calculated to determine significant relationships between DC density, nerve parameters, duration of infection, and patient age. Differences were considered statistically significant for *P* values < 0.05. Analyses were performed with statistical analysis software (SAS software version 9.2; SAS Institute Inc., Cary, NC).

## RESULTS

Fifty-three eyes of 53 patients with IK including bacterial (*n* = 23), fungal (*n* = 13) and *Acanthamoeba* (*n* = 17) (Figs. 3A–C) infection were included for analysis and were compared with 20 eyes of 20 normal volunteers. Demographic data of the IK subgroups and control group are presented in Table 1.

### Corneal Subbasal Nerve Plexus by IVCN

Quantitative analysis of nerve parameters for IK subgroups and normal control group are in Table 2. Patients with IK showed a significant reduction in the subbasal nerve plexus parameters when compared with controls (Fig. 2 and Figs. 3G, 3K, and 3L–N). In particular, the mean nerve density ( $674.2 \pm 976.1$  vs.

$3913.9 \pm 507.4$   $\mu\text{m}/\text{frame}$ ; *P* < 0.0001), the total number of nerves ( $2.7 \pm 3.9$  vs.  $20.2 \pm 3.3$ ; *P* < 0.0001), the number of main nerve trunks ( $1.5 \pm 2.2$  vs.  $6.9 \pm 1.1$ ; *P* < 0.0001), and the number of branches ( $1.2 \pm 2.0$  vs.  $13.5 \pm 3.1$ ; *P* < 0.0001) were all found to be significantly lower. Nerve tortuosity was increased in IK eyes when compared with controls, but did not reach statistical significance ( $1.7 \pm 1.3$  vs.  $1.1 \pm 0.5$ ; *P* = 0.06).

Furthermore, subgroup analysis of patients with IK demonstrated that patients with bacterial (Fig. 3L), fungal (Fig. 3M), and *Acanthamoeba* (Fig. 3N) keratitis all had a significantly reduced subbasal nerve plexus compared with controls, including the mean nerve density ( $824.0 \pm 1050.7$ ,  $956.9 \pm 1093.0$ ,  $215.6 \pm 575.4$ , respectively, vs.  $3913.9 \pm 507.4$   $\mu\text{m}/\text{frame}$ ; *P* < 0.0001), the total number of nerves ( $3.4 \pm 4.5$ ,  $3.9 \pm 4.6$ ,  $0.5 \pm 1.0$ , respectively, vs.  $20.2 \pm 3.3$ ; *P* < 0.0001), the number of main nerve trunks ( $1.9 \pm 2.5$ ,  $2.0 \pm 2.3$ ,  $0.5 \pm 1.1$ , respectively, vs.  $6.9 \pm 1.1$ ; *P* < 0.0001), and the number of branches ( $1.5 \pm 2.3$ ,  $0.9 \pm 1.7$ ,  $0.3 \pm 0.9$ , respectively, vs.  $13.5 \pm 3.1$ ; *P* < 0.0001; Fig. 2). Comparison between subgroups demonstrated that the *Acanthamoeba* keratitis group showed a more profound decrease in nerve parameters when compared with the bacterial and fungal subgroups, some of which reached statistical significance (Table 2).

### Dendritic Cells by IVCN

Dendritic-shaped cells (DCs) were located on the subbasal layer in close proximity to the nerve plexus (Fig. 1, and Figs. 3G–K), with an average distance between DCs and nerves of  $13.6 \pm 5.5$   $\mu\text{m}$  and a range of 0 to 26  $\mu\text{m}$ . Quantitative analysis of the DC density, DC size, and number of dendrites per cell for IK subgroups and the normal control group is shown in Table 2. We observed central epithelial DCs in 100% of normal corneas, with a mean density of  $49.3 \pm 39.6$  cells/ $\text{mm}^2$  (Figs.

TABLE 2. Corneal Subbasal Nerve Plexus Parameters and Dendritic Cell Density in Infectious Keratitis

	Infectious Keratitis Patients			
	Bacterial	Fungal	Acanthamoeba	Controls
Eyes, <i>n</i>	23	13	17	20
Dendritic cell density, cells/ $\text{mm}^2$	$441.1 \pm 320.5^{\dagger}$	$608.9 \pm 812.5^*$	$1000.2 \pm 1090.3^*$	$49.3 \pm 39.6$
Dendritic cell area, $\mu\text{m}^2$	$195.3 \pm 98.5^*$	$276.5 \pm 160.7^*$	$170.1 \pm 54.4^*$	$81.6 \pm 23.8$
Number of dendrites, dendrites/cell	$5.1 \pm 1.9^*$	$4.5 \pm 1.1^*$	$4.2 \pm 0.5^*$	$3.0 \pm 0.4$
Subbasal nerve density, $\mu\text{m}/\text{frame}$	$824.0 \pm 1,050.7$	$956.9 \pm 1,093.0$	$215.6 \pm 575.4$	$3,913.9 \pm 507.4$
[ $\mu\text{m}/\text{mm}^2$ ]	$[5,150 \pm 6,566]^*$	$[5,980 \pm 6,831]^{\dagger}$	$[1,347 \pm 3,596]^*$	$[24,461 \pm 3,171]$
Total nerves, <i>n</i>	$3.4 \pm 4.5^{\dagger}$	$3.9 \pm 4.6^{\dagger}$	$0.5 \pm 1.0^*$	$20.0 \pm 3.7$
Main nerve trunks, <i>n</i>	$1.9 \pm 2.5^{\dagger}$	$2.0 \pm 2.3^{\dagger}$	$0.5 \pm 1.1^*$	$6.7 \pm 1.2$
Total nerve branches, <i>n</i>	$1.5 \pm 2.3^*$	$0.9 \pm 1.7^*$	$0.3 \pm 0.9^*$	$13.4 \pm 3.4$
Grade of tortuosity	$1.9 \pm 1.3^*$	$1.1 \pm 1.1$	$1.8 \pm 1.6$	$1.1 \pm 0.5$

Values reported as mean ± SD.

\* Statistically significant (*P* < 0.05) compared with controls.

† Statistically significant (*P* < 0.05) compared with the *Acanthamoeba* subgroup.



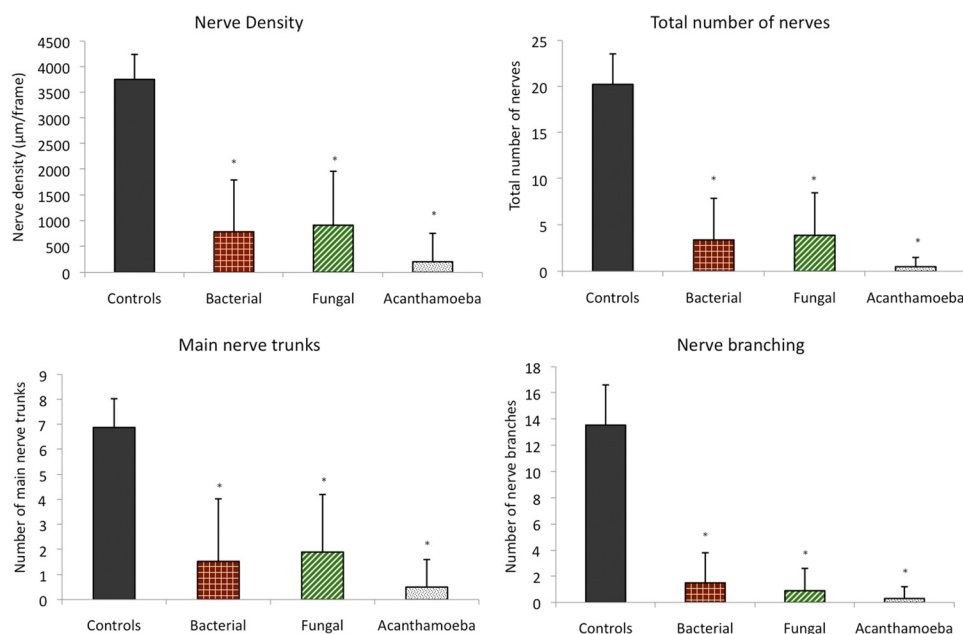


**FIGURE 2.** Corneal nerve parameters in infectious keratitis patients. Bacterial, fungal, and *Acanthamoeba* keratitis patients showed statistical significant diminishment of corneal nerve parameters compared with controls. No significant difference was found between the different etiologies of infection. (A) Nerve density. (B) Total number of nerves. (C) Main nerve trunks. (D) Nerve branching. Error bars represent SD from the mean. Statistical analysis by ANOVA. \* $P < 0.0001$  compared with control group.

3G–K). No statistically significant relationship between DC density with age or sex was detected ( $P = 0.59$ ;  $R = 0.06$ ).

Patients with IK showed a significant increase in DC density when compared with controls ( $672.9 \pm 791.5$  vs.  $49.3 \pm 39.6$ ;  $P < 0.0001$ ), which was significantly more pronounced for *Acanthamoeba* keratitis ( $1000.2 \pm 1090.3$ ) (Figs. 3F and 3J) compared with bacterial ( $441.1 \pm 320.5$ ,  $P < 0.02$ ) (Figs. 3D and 3H), but not fungal keratitis ( $608.9 \pm 812.5$ ) (Figs. 3E and 3I) (Fig. 4). Further, IVCN revealed morphologic changes in DCs in all IK subgroups. While small cells with few if any dendrites (presumably immature) were present in normal corneas, patients with IK demonstrated a clear increase in both size of DCs ( $233 \pm 108.4 \mu\text{m}^2$  vs.  $81.6 \pm 23.8 \mu\text{m}^2$ ,  $P < 0.001$ ), and number of dendritic processes compared with controls ( $4.6 \pm 0.9$  vs.  $3.0 \pm 0.4$  dendrites per cell;  $P < 0.001$ ), presumably characteristics of a more mature phenotype.

### Correlation of Dendritic Cell Density and Subbasal Corneal Nerve Alterations

The increase in DC density was significantly correlated to the substantial diminishment of subbasal corneal nerves in patients with IK ( $R = -0.44$ ;  $P < 0.0005$ ) (Fig. 5A). Similarly, the increase in DC density was significantly correlated with the loss of main nerve trunks ( $R = -0.41$ ;  $P < 0.002$ ), total number of nerves ( $R = -0.39$ ;  $P < 0.002$ ), and nerve branches ( $R = -0.39$ ;  $P < 0.003$ ) (Figs. 5B–D). We neither found a significant correlation between the IVCN findings and age ( $R = 0.06$ ;  $P = 0.59$ ), nor with the duration of infection ( $R = -0.21$ ;  $P = 0.19$ ).

### DISCUSSION

The assessment of corneal innervation and inflammation, until recently, has only been possible through the measurement of corneal sensation and slit-lamp biomicroscopy, respectively. The use of rapid, noninvasive in vivo confocal microscopy now allows systematic studies of corneal nerve morphology and density, as well as the study of immune cells (including dendritic cells) in patients. Our study presented herein, is the largest prospective IVCN study performed in patients with bacterial, fungal, and *Acanthamoeba* keratitis. To our knowledge, this is the first study to systematically analyze subbasal

nerve changes, epithelial DC changes, and their potential correlation in infectious keratitis.

In the present study, we demonstrate a significant decrease of the subbasal nerve density in patients with IK ( $4213 \pm 6100$  vs.  $24,461 \pm 3171 \mu\text{m}/\text{mm}^2$ ). Subbasal nerve density varies depending on the type of confocal microscope used (reviewed in Ref. 25). Subbasal corneal nerve density in normal eyes range between  $5534 \mu\text{m}/\text{mm}^2$  and  $10,658 \mu\text{m}/\text{mm}^2$  using the tandem scanning confocal microscope (TSCM) and slit scanning confocal microscope (SSCM), respectively.<sup>26</sup> In contrast, a study by Patel et al.<sup>27</sup> demonstrated the subbasal nerve density to be as high as  $21,668 \mu\text{m}/\text{mm}^2$  using the laser scanning confocal microscope (LSCM), which is comparable with our results in normal corneas.

Recently, we demonstrated a significant decrease in corneal innervation by IVCN (Confoscan 4; Nidek Inc.) in patients with HSK, which strongly correlated with the loss of corneal sensitivity.<sup>6</sup> Although our current results are not directly comparable with this report due to the use of different technologies, the level of decrease in subbasal nerves seems to be more profound than in HSK. Historically, clinicians measure corneal sensation to differentiate HSK from other sources of IK. Our current report, however, suggests that bacterial, fungal, and *Acanthamoeba* keratitis all result, at least temporarily, in neurotrophic keratopathy as well. Prospective longitudinal studies are currently underway to demonstrate whether these changes in the subbasal plexus are permanent or temporary.

Interestingly, although the diminishment of the subbasal nerve plexus was noted in all subgroups, this was more severe in the *Acanthamoeba* group. This trend could not entirely be ascribed to the potentially longer duration of disease, which was similar between the fungal and the *Acanthamoeba* groups. In addition, perineuritis, a hallmark of *Acanthamoeba* keratitis,<sup>28</sup> could have led to this observation. Further, a study by Pettit et al.<sup>29</sup> demonstrated that *Acanthamoeba* trophozoites were able to destroy nerve cells in vitro both by cytolysis and by ingestion. Alternatively, diminishment in corneal innervation could be directly related to the level of inflammation, which is typically more profound in patients with *Acanthamoeba* and fungal keratitis. Reduced subbasal nerve density in noninfectious inflammatory diseases has previously been described such as in dry eye syndrome,<sup>30–33</sup> with a length per

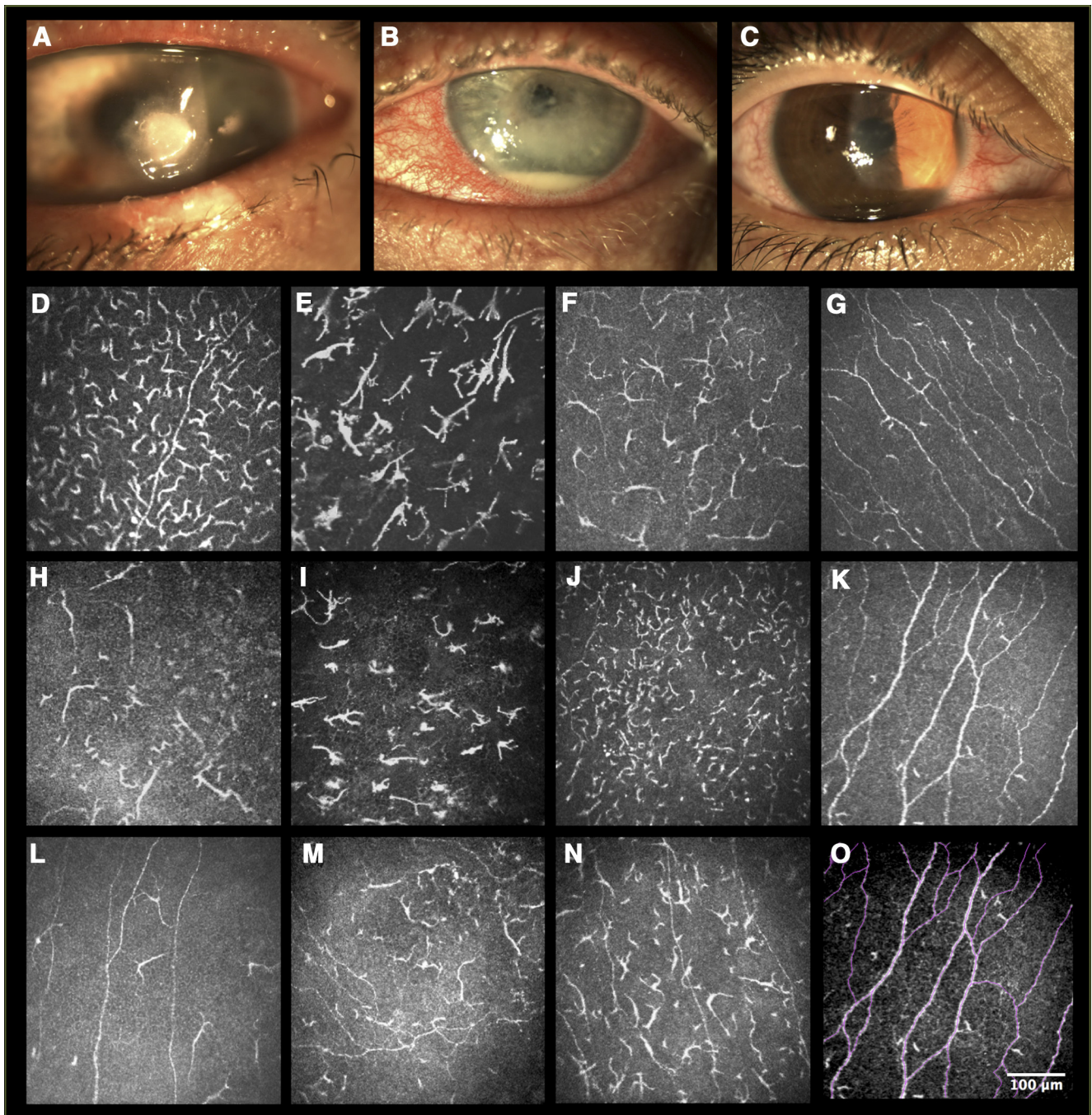


**FIGURE 3.** Corneal subbasal nerve plexus and dendritic cells. (A) Slit lamp photo of bacterial keratitis. (B) Slit lamp photo of fungal keratitis. (C) Slit lamp photo of *Acanthamoeba* keratitis. (D–O) In vivo confocal microscopy images. (D, H) Bacterial keratitis. (E, I) Fungal keratitis. (F, J) *Acanthamoeba* keratitis. (G, K) Normal control. (L, M, N) Decreased subbasal nerve plexus in bacterial, fungal, and *Acanthamoeba* keratitis, respectively. Reduction of the subbasal nerve plexus with increased density of the dendritic cells is observed in the different groups of infectious keratitis. (O) NeuronJ tracings in normal control subbasal nerve plexus.

frame of  $511 \pm 106 \mu\text{m}/\text{frame}$  by slit-scanning confocal microscope, although not to the level observed in our present study. Together, these findings suggest that any inflammatory process could potentially lead to loss of corneal innervation and might potentially result in neurotrophic keratopathy.

Laser IVCN reveals the presence of corneal epithelial dendritiform cells. Dendritiform cells observed in the corneal epithelium by IVCN cannot categorically be defined as DC based on morphology alone, as macrophages, for example, can obtain a dendritic morphology as well. However, previous studies

in mice and human corneas by our group and other laboratories<sup>10,12,13,15,34,35</sup> have clearly demonstrated that the bone marrow-derived cells present in the normal corneal epithelium are exclusively dendritic cells. A recent study by Guthoff et al.<sup>36</sup> has compared ex vivo and in vivo morphology of different leukocytes. They have shown that while laser scanning confocal microscope does not allow the clinician to distinguish cell characteristics, such as the presence of nucleoli or granules, the typical cell morphology, diameter of the cell body, and location of the cell, all may aid the clinician in the correct



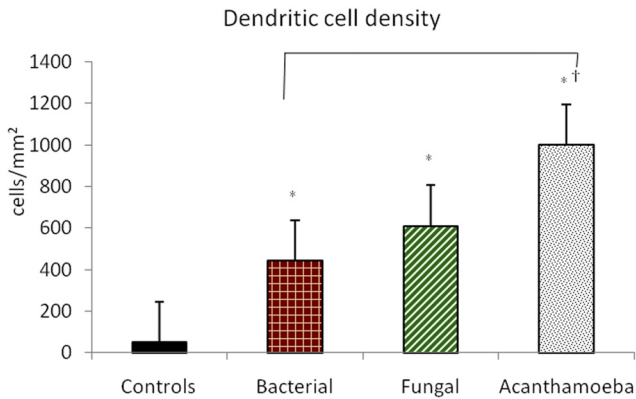


**FIGURE 4.** Dendritic cell density in infectious keratitis patients. Patients with bacterial, fungal, and *Acanthamoeba* keratitis had significantly higher epithelial dendritic cell density than control subjects. Error bars represent SE from the mean. \* $P < 0.0001$  compared with control group. † $P < 0.0001$  bacterial compared with *Acanthamoeba* group. Statistical analysis by ANOVA.

interpretation of the confocal data. This group demonstrated that granular leukocytes such as neutrophils, basophils, and eosinophils are  $<10$  microns in size, while nongranular leukocytes, such as lymphocytes and monocytes are up to 15 microns and 20 microns respectively. Thus, while the cells we counted could in theory be other inflammatory cells, the morphology (bean-shape), dendrites, lack of several nuclear lobes, and larger size, suggest that these cells could be monocytes, tissue macrophages, but most likely dendritic cells of the epithelium.

We observed the presence of DCs in normal controls ( $49.3 \pm 39.6$  cells/mm<sup>2</sup>) in close proximity to nerves, which has previously been noted ex vivo.<sup>37–40</sup> Previous IVCN studies have shown the presence of epithelial DCs (24.1 cells/mm<sup>2</sup> and 34.9 cells/mm<sup>2</sup>)<sup>16–18</sup> in the central cornea of 20.0%<sup>17</sup> to 31.3%<sup>16</sup> healthy volunteers. In patients with IK, we found a significant increase in DC density, regardless of etiology. Further, while DCs in central normal corneas are smaller in size with few if any dendrites (presumably immature), patients with IK demonstrate a significant increase in both size of DCs, as well as in the number of dendrites. The variable appearance of DCs possibly indicates different stages of maturation or activation of these cells. These findings are in agreement with prior IVCN studies and numerous ex vivo studies in mice demonstrating that while the corneal center is comprised almost entirely of immature and precursor DCs,<sup>8,10,11,15,41,42</sup> during inflammation there is an increase in mature DCs.<sup>34</sup> The relatively wide range in DC density ( $672.9 \pm 791.5$  cells/mm<sup>2</sup>) could also be explained by the variation in the level of corneal inflammation and associated proinflammatory cytokines and chemokines across the patients. Interestingly, the *Acanthamoeba* keratitis subgroup had a significantly higher DC density than the bacterial keratitis group. While this could potentially be related to the more profound loss of nerves in this group, it could alternatively be attributable to more severe inflammation observed in the amoeba group as well. Moreover, this difference

could be due to the fact that patients with fungal and *Acanthamoeba* keratitis were not treated with steroids, while some patients with bacterial keratitis did receive steroid treatment.

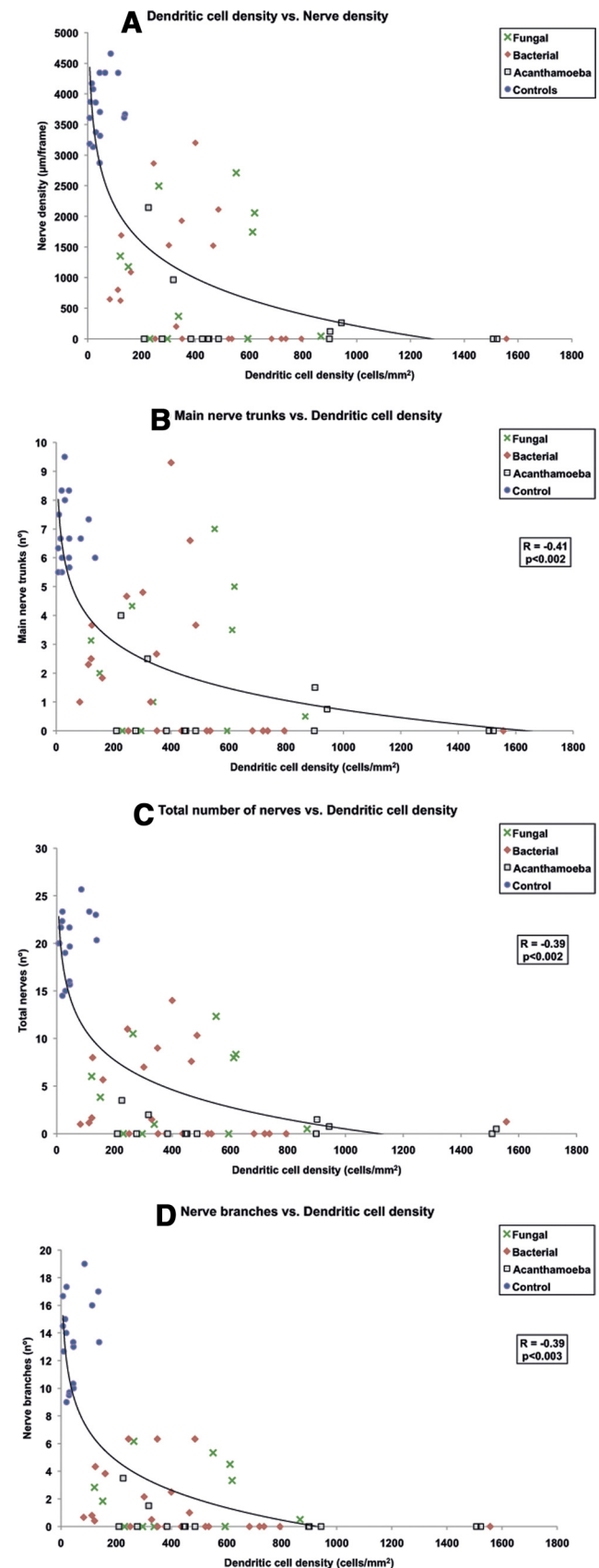


**FIGURE 5.** Correlation between dendritic cell density increase and corneal nerve diminishment. Multivariate regression factor and  $P$  values are shown. Dendritic cell density is significantly correlated to nerve density (A), main nerve trunks (B), total number of nerves (C), and nerve branches (D). Three outlier patients with the highest dendritic cell density and no nerves (4847.1; 3194.0; 2608.0) are not plotted in the figures because they are outside the highest limit of the axis.

Increased density of corneal DCs by IVCN has previously been described in patients with dry eye,<sup>18</sup> in immune-mediated inflammatory diseases,<sup>17</sup> and in patients with pterygia.<sup>43,44</sup> While Lin et al.<sup>18</sup> demonstrated an epithelial DC density of  $89.8 \pm 10.8$  and  $127.9 \pm 23.7$  cells/mm<sup>2</sup> in 32 non-Sjögren's and 14 Sjögren's patients respectively, Mastropasqua et al.<sup>17</sup> demonstrated a DC density of  $194 \pm 76.2$  cells/mm<sup>2</sup> in 45 eyes with vernal keratoconjunctivitis, adenoviral keratitis, corneal graft rejection, and recurrent stromal HSK. Further, Labbé et al.<sup>43</sup> and Wang et al.<sup>44</sup> demonstrated increased DC density in eyes with pterygia. Moreover, increased DC density has been observed in 16 eyes with viral keratitis,<sup>45</sup> three eyes with Thygeson's keratitis,<sup>46</sup> a patient with deep lamellar keratitis after LASIK,<sup>47</sup> and a patient with bacterial keratitis.<sup>48</sup> While the DC density in some patients in our IK groups are comparable with the study by Mastropasqua et al.<sup>17</sup> the overall DC density is 2- to 5-fold higher.

We feel that several factors are important in obtaining high-quality, artifact-free images with the confocal microscope used in this study (Heidelberg Retina Tomograph 3 with the Rostock Cornea Module, Heidelberg Engineering GmbH) particularly in patients with IK. These include well-trained personnel, patient collaboration, improved optical coupling of the cap to the corneal surface with additional drop of hydroxypropyl methylcellulose 2.5% on the outside tip of the cap, and finally the use of sequence scans for imaging the layers of interest. Further, in case folds or artifacts are encountered, gentle retraction of the cap reduces pressure on the cornea and may resolve artifacts. Moreover, sequential sequence scans performed in and around the corneal ulcer or infiltrate, focusing on the same layer are crucial to provide sufficient time for the machine to adjust the contrast according to the reflectivity of the tissue and obtain sufficient high-quality representative images.

The increase in central epithelial DCs herein was strongly associated with the diminishment of the subbasal nerve density and numbers, suggesting a potential interplay between the immune and nervous system in the cornea. We acknowledge the limitations of in vivo studies in patients to determine the exact nature of the inverse relationship of DC density and subbasal nerve number and density demonstrated here. While theoretically these events could be partially or completely independent, our preliminary preclinical animal studies suggest that these events are, at least in part, directly related. This communication is likely maintained through a biochemical language, with cytokines produced by immune cells being recognized by receptors on cells of the neuroendocrine system, and vice versa, with cells of the immune system recognizing neurotransmitters and neuropeptides produced by the nerves.<sup>49</sup> For example, Hosoi et al. have shown that calcitonin gene-related peptide (CGRP) was able to directly inhibit antigen presentation by epidermal Langerhans cells.<sup>50</sup> Interestingly, while the cornea, an immune-privileged tissue, has the highest nerve density in the whole body with a density 300 times higher than the skin, the DC density in the central cornea is extremely low under steady state conditions with  $49.3 \pm 39.6$ /mm<sup>2</sup> in the central cornea versus  $378 \pm 20$ /mm<sup>2</sup> in the epidermis (a level similar to the DC density in bacterial keratitis).<sup>51</sup> Further, the low nerve number and density in our patients with IK, is still several fold higher than the nerve density of the skin. Thus, the concurrent demonstration of higher DC density and decrease in nerve density is not necessarily surprising.

Further, substance P (SP), expressed by enteric neurons, has been shown to modulate colonic inflammation in the gut.<sup>52</sup> Moreover, the immunomodulatory and tolerogenic effect of various neuropeptides have been suggested,<sup>53</sup> which, in their absence due to damage to nerves could lead to enhanced immune response as seen in our study. In the cornea, Hazlett's group has recently demonstrated the role of substance P in

IFN- $\gamma$  production of natural killer cells,<sup>54</sup> and the immunomodulatory function of vasoactive intestinal peptide (VIP) in the murine *Pseudomonas aeruginosa* keratitis model through regulation of adhesion molecule expression.<sup>55,56</sup> It has been suggested that the immune system may act as a "sixth sense," informing the nervous system that a systemic immune/inflammatory response to infection or tissue injury is occurring.<sup>57</sup> Thus, it is tempting to speculate that in the setting of infectious corneal diseases and the loss of immune privilege, the increased presence of DC could serve to protect the cornea in the absence of fully functional protection by corneal nerves.

A limitation of the present study is that the IVCN only provides morphologic and morphometric data on cells and nerves. Due to the "in vivo" nature of this study in patients, functional data cannot be demonstrated. Animal studies are currently underway to elucidate the mechanisms of our findings. In addition, by evaluating only the center of the cornea for corneal nerves and DC, we cannot necessarily extrapolate our findings to the peripheral cornea. Further, poor topographic reproducibility and the difficulty to ensure the exact same locations are tested in all patients are currently not optimal. However, as the differences between the control and IK groups are dramatic, this will likely not alter the conclusions of this study.

In conclusion, IVCN enables a direct and reproducible observation of increased corneal epithelial DC at the level of the subbasal nerve plexus, and demonstrates strong correlation with the profound loss of the subbasal nerve plexus. Additional studies are needed to demonstrate if the loss of subbasal nerve plexus in these patients will lead to loss of corneal sensation, in which case the role of measuring corneal sensitivity to distinguish HSK from other forms of IK would need to be reconsidered, as it could lead to erroneous conclusions and management of these patients. Further, the study of corneal innervation by IVCN demonstrates an objective methodology for monitoring patients, potentially predicting the risk of neurotrophic keratopathy. Quantification of DC and other immune cells by IVCN could potentially allow objective evaluation of antimicrobial and anti-inflammatory treatment response in the cornea.

## References

1. Beuerman RW, Schimmelpfennig B. Sensory denervation of the rabbit cornea affects epithelial properties. *Exp Neurol*. 1980;69:196-201.
2. Stern ME, Beuerman RW, Fox RI, Gao J, Mircheff AK, Pflugfelder SC. The pathology of dry eye: the interaction between the ocular surface and lacrimal glands. *Cornea*. 1998;17:584-589.
3. Müller LJ, Pels L, Vrensen GF. Ultrastructural organization of human corneal nerves. *Invest Ophthalmol Vis Sci*. 1996;37:476-488.
4. Cruzat A, Pavan-Langston D, Hamrah P. In vivo confocal microscopy of corneal nerves: analysis and clinical correlation. *Semin Ophthalmol*. 2010;25:171-177.
5. Patel DV, McGhee CN. In vivo confocal microscopy of human corneal nerves in health, in ocular and systemic disease, and following corneal surgery: a review. *Br J Ophthalmol*. 2009;93:853-860.
6. Hamrah P, Cruzat A, Dastjerdi MH, et al. Corneal sensation and subbasal nerve alterations in patients with herpes simplex keratitis: an in vivo confocal microscopy study. *Ophthalmology*. 2010;117:1930-1936.
7. Steinman RM, Banchereau J. Taking dendritic cells into medicine. *Nature*. 2007;449:419-426.
8. Hamrah P, Dana MR. Corneal antigen-presenting cells. *Chem Immunol Allergy*. 2007;92:58-70.
9. Hamrah P, Dana MR. Antigen-presenting cells in the eye and ocular surface. In: Dartt DA, ed. *Encyclopedia of the Eye*. Vol 1. Oxford: Academic Press; 2010:120-127.
10. Hamrah P, Zhang Q, Liu Y, Dana MR. Novel characterization of MHC class II-negative population of resident corneal Langerhans cell-type dendritic cells. *Invest Ophthalmol Vis Sci*. 2002;43:639-646.



11. Hamrah P, Liu Y, Zhang Q, Dana MR. The corneal stroma is endowed with significant numbers of resident dendritic cells. *Invest Ophthalmol Vis Sci.* 2003;44:581-589.
12. Nakamura T, Ishikawa F, Sonoda KH, et al. Characterization and distribution of bone marrow-derived cells in the mouse cornea. *Invest Ophthalmol Vis Sci.* 2005;46:497-503.
13. Yamagami S, Yokoo S, Usui T, Yamagami H, Amano S, Ebihara N. Distinct populations of dendritic cells in the normal human donor corneal epithelium. *Invest Ophthalmol Vis Sci.* 2005;46:4489-4494.
14. Yamagami S, Ebihara N, Usui T, Yokoo S, Amano S. Bone marrow-derived cells in normal human corneal stroma. *Arch Ophthalmol.* 2006;124:62-99.
15. Mayer WJ, Irschick UM, Moser P, et al. Characterization of antigen-presenting cells in fresh and cultured human corneas using novel dendritic cell markers. *Invest Ophthalmol Vis Sci.* 2007;48:4459-4467.
16. Zhivov A, Stave J, Vollmar B, Guthoff R. In vivo confocal microscopic evaluation of Langerhans cell density and distribution in the normal human corneal epithelium. *Graefes Arch Clin Exp Ophthalmol.* 2005;243:1056-1061.
17. Mastropasqua L, Nubile M, Lanzini M, et al. Epithelial dendritic cell distribution in normal and inflamed human cornea: in vivo confocal microscopy study. *Am J Ophthalmol.* 2006;142:736-744.
18. Lin H, Li W, Dong N, et al. Changes in corneal epithelial layer inflammatory cells in aqueous tear-deficient dry eye. *Invest Ophthalmol Vis Sci.* 2010;51:122-128.
19. Sirinek LP, O'Dorisio MS. Modulation of immune function by intestinal neuropeptides. *Acta Oncol.* 1991;30:509-517.
20. McGillis JP, Mitsuhashi M, Payan DG. Immunomodulation by tachykinin neuropeptides. *Ann NY Acad Sci.* 1990;594:85-94.
21. Rabin BS, Cohen S, Ganguli R, Lysle DT, Cunnick JE. Bidirectional interaction between the central nervous system and the immune system. *Crit Rev Immunol.* 1989;9:279-312.
22. Calvillo MP, McLaren JW, Hodge DO, Bourne WM. Corneal reinnervation after LASIK: prospective 3-year longitudinal study. *Invest Ophthalmol Vis Sci.* 2004;45:3991-3996.
23. Meijering E, Jacob M, Sarria JC, Steiner P, Hirling H, Unser M. Design and validation of a tool for neurite tracing and analysis in fluorescence microscopy images. *Cytometry A.* 2004;58:167-176.
24. Oliveira-Soto L, Efron N. Morphology of corneal nerves using confocal microscopy. *Cornea.* 2001;20:374-384.
25. Erie JC, McLaren JW, Patel SV. Confocal microscopy in ophthalmology. *Am J Ophthalmol.* 2009;148:639-646.
26. Erie EA, McLaren JW, Kittleson KM, Patel SV, Erie JC, Bourne WM. Corneal subbasal nerve density: a comparison of two confocal microscopes. *Eye Contact Lens.* 2008;34:322-325.
27. Patel DV, McGhee CN. Mapping of the normal human corneal sub-basal nerve plexus by in vivo laser scanning confocal microscopy. *Invest Ophthalmol Vis Sci.* 2005;46:4485-4488.
28. Pfister DR, Cameron JD, Krachmer JH, Holland EJ. Confocal microscopy findings of Acanthamoeba keratitis. *Am J Ophthalmol.* 1996;121:119-128.
29. Pettit DA, Williamson J, Cabral GA, Marciano-Cabral F. In vitro destruction of nerve cell cultures by Acanthamoeba spp.: a transmission and scanning electron microscopy study. *J Parasitol.* 1996;82:769-777.
30. Tuisku IS, Kontinen YT, Kontinen LM, Tervo TM. Alterations in corneal sensitivity and nerve morphology in patients with primary Sjögren's syndrome. *Exp Eye Res.* 2008;86:879-885.
31. Benítez-Del-Castillo JM, Acosta MC, Wassfi MA, et al. Relation between corneal innervation with confocal microscopy and corneal sensitivity with noncontact esthesiometry in patients with dry eye. *Invest Ophthalmol Vis Sci.* 2007;48:173-181.
32. Villani E, Galimberti D, Viola F, Mapelli C, Ratiglia R. The cornea in Sjögren's syndrome: an in vivo confocal study. *Invest Ophthalmol Vis Sci.* 2007;48:2017-2022.
33. Hosai BM, Ornek N, Zilelioglu G, Elhan AH. Morphology of corneal nerves and corneal sensation in dry eye: a preliminary study. *Eye.* 2005;19:1276-1279.
34. Hamrah P, Liu Y, Zhang Q, Dana MR. Alterations in corneal stromal dendritic cell phenotype and distribution in inflammation. *Arch Ophthalmol.* 2003;121:1132-1140.
35. Knickelbein JE, Watkins SC, McMenamin PG, Hendricks RL. Stratification of antigen-presenting cells within the normal cornea. *Ophthalmol Eye Dis.* 2009;1:45-54.
36. Guthoff RF, Zhivov A, Stachs O. In vivo confocal microscopy, an inner vision of the cornea - a major review. *Clin Experiment Ophthalmol.* 2009;37:100-117.
37. Scharenberg K. The cells and nerves of the human cornea: a study with silver carbonate. *Am J Ophthalmol.* 1955;40:368-379.
38. Pau H, Conrads H. Significance of the Langerhans cells for the nerves of the corneal epithelium. *Albrecht Von Graefes Arch Ophthalmol.* 1957;158:427-433.
39. Schimmelpfennig B. Nerve structures in human central corneal epithelium. *Graefes Arch Clin Exp Ophthalmol.* 1982;218:14-20.
40. He J, Bazan NG, Bazan HE. Mapping the entire human corneal nerve architecture. *Exp Eye Res.* 2010;91:513-523.
41. Zhivov A, Stachs O, Kraak R, Stave J, Guthoff RF. In vivo confocal microscopy of the ocular surface. *Ocul Surf.* 2006;4:81-93.
42. Hamrah P, Huq SO, Liu Y, Zhang Q, Dana MR. Corneal immunity is mediated by heterogeneous population of antigen-presenting cells. *J Leukoc Biol.* 2003;74:172-178.
43. Labbé A, Gheck L, Iordanidou V, Mehanna C, Brignole-Baudouin F, Baudouin C. An in vivo confocal microscopy and impression cytology evaluation of pterygium activity. *Cornea.* 2010;29:392-399.
44. Wang Y, Zhao F, Zhu W, Xu J, Zheng T, Sun X. In vivo confocal microscopic evaluation of morphologic changes and dendritic cell distribution in pterygium. *Am J Ophthalmol.* 2010;150:650-655.
45. Rosenberg ME, Tervo TM, Müller LJ, Moilanen JA, Vesaluoma MH. In vivo confocal microscopy after herpes keratitis. *Cornea.* 2002;21:265-269.
46. Kawamoto K, Chikama T, Takahashi N, Nishida T. In vivo observation of Langerhans cells by laser confocal microscopy in Thygeson's superficial punctate keratitis. *Mol Vis.* 2009;15:1456-1462.
47. Hadden OB, Patel D, Gray TB, Morris AT, Ring CP. Multifocal lamellar keratitis following laser in situ keratomileusis. *J Cataract Refract Surg.* 2007;33:144-147.
48. Su PY, Hu FR, Chen YM, Han JH, Chen WL. Dendritiform cells found in central cornea by in-vivo confocal microscopy in a patient with mixed bacterial keratitis. *Ocul Immunol Inflamm.* 2006;14:241-244.
49. Sternberg EM. Neural regulation of innate immunity: a coordinated nonspecific host response to pathogens. *Nat Rev Immunol.* 2006;6:318-328.
50. Hosoi J, Murphy GF, Egan CL, et al. Regulation of Langerhans cell function by nerves containing calcitonin gene-related peptide. *Nature.* 1993;363:159-163.
51. Smolle J, Soyer HP, Ehall R, Bartenstein S, Kerl H. Langerhans cell density in epithelial skin tumors correlates with epithelial differentiation but not with the peritumoral infiltrate. *J Invest Dermatol.* 1986;87:477-479.
52. Koon HW, Pothoulakis C. Immunomodulatory properties of substance P: the gastrointestinal system as a model. *Ann NY Acad Sci.* 2006;1088:23-40.
53. Gonzalez-Rey E. Keeping the balance between immune tolerance and pathogen immunity with endogenous neuropeptides. *Neuroimmunomodulation.* 2010;17:161-164.
54. Lighvani S, Huang X, Trivedi PP, Swanborg RH, Hazlett LD. Substance P regulates NK cell IFN production and resistance to Pseudomonas aeruginosa infection. *Eur J Immunol.* 2005;35:1567-1575.
55. Szliter EA, Lighvani S, Barrett RP, Hazlett LD. Vasoactive intestinal peptide balances pro- and anti-inflammatory cytokines in the Pseudomonas aeruginosa infected cornea and protects against corneal perforation. *J Immunol.* 2007;178:1105-1114.
56. Berger EA, McClellan SA, Barrett RP, Hazlett LD. VIP promotes resistance in the Pseudomonas aeruginosa-infected cornea by modulating adhesion molecule expression. *Invest Ophthalmol Vis Sci.* 2010;51:5776-5782.
57. Gonzalez-Rey E, Ganea D, Delgado M. Neuropeptides: keeping the balance between pathogen immunity and immune tolerance. *Curr Opin Pharmacol.* 2010;10:1-9.